

Zero-temperature coarsening in the 2d Potts model

This content has been downloaded from IOPscience. Please scroll down to see the full text.

J. Stat. Mech. (2013) P06018

(<http://iopscience.iop.org/1742-5468/2013/06/P06018>)

View [the table of contents for this issue](#), or go to the [journal homepage](#) for more

Download details:

IP Address: 155.41.111.161

This content was downloaded on 26/09/2013 at 16:14

Please note that [terms and conditions apply](#).

Zero-temperature coarsening in the 2d Potts model

J Olejarz¹, P L Krapivsky² and S Redner¹

¹ Center for Polymer Studies and Department of Physics, Boston University, Boston, MA 02215, USA

² Department of Physics, Boston University, Boston, MA 02215, USA

E-mail: jasonolejarz@gmail.com, paulk@bu.edu and redner@buphy.bu.edu

Received 11 May 2013

Accepted 5 June 2013

Published 27 June 2013

Online at stacks.iop.org/JSTAT/2013/P06018

doi:10.1088/1742-5468/2013/06/P06018

Abstract. We study the fate of the 2d kinetic q -state Potts model after a sudden quench to zero temperature. Both ground states and complicated static states are reached with non-zero probabilities. These outcomes resemble those found in the quench of the 2d Ising model; however, the variety of static states in the q -state Potts model (with $q \geq 3$) is much richer than in the Ising model, where static states are either ground or stripe states. Another possibility is that the Potts system gets trapped on a set of equal-energy blinker states, where a subset of spins can flip *ad infinitum*; these states are similar to those found in the quench of the 3d Ising model. The evolution towards the final energy is also unusual—at long times, sudden and massive energy drops may occur that are accompanied by macroscopic reordering of the domain structure. This indeterminacy in the zero-temperature quench of the kinetic Potts model is at odds with basic predictions from the theory of phase-ordering kinetics. We also propose a continuum description of coarsening with more than two equivalent ground states. The resulting time-dependent Ginzburg–Landau equations reproduce the complex cluster patterns that arise in the quench of the kinetic Potts model.

Keywords: coarsening processes (theory)

ArXiv ePrint: [1305.1038](https://arxiv.org/abs/1305.1038)

Contents

1. Introduction	2
2. Models	7
2.1. Kinetic Potts model	7
2.2. Time-dependent Ginzburg–Landau (TDGL) equation	7
3. Non-symmetric initial conditions	9
4. Cluster geometry at long time	11
4.1. Kinetic Potts model	11
4.2. TDGL equation.	13
5. Ultra-slow evolution	14
6. Avalanche dynamics for large q	17
7. Discussion	19
Acknowledgments	21
References	22

1. Introduction

What happens when a system with degenerate ground states is suddenly quenched from an initial supercritical temperature, $T_i > T_c$, to a final subcritical temperature, $0 \leq T_f < T_c$? The answer to this question depends on the temperatures T_i and T_f , the spatial dimension d , and the dynamics. Numerous studies of systems with two degenerate ground states, particularly the Ising model, revealed that the qualitative behaviors are remarkably universal and depend only on basic features of the dynamics (see, e.g., [1]–[3] and references therein). For spin systems, this universality allows us to consider the simplest microscopic single spin-flip dynamics, leading to what is known as the kinetic Ising model. A more macroscopic approach is based on the Landau free-energy functional with a potential that has two degenerate minima. The corresponding non-conservative dynamics is the time-dependent Ginzburg–Landau (TDGL) equation for a scalar order parameter [1]–[3].

Both for the kinetic Ising model and the TDGL equation, an intricate coarsening domain mosaic emerges shortly after the quench. This mosaic has a characteristic length scale that grows in time as $t^{1/2}$. Because the dynamics is universal for all subcritical quenches, we focus on quenches to zero temperature, $T_f = 0$. In this limit, the early-time evolution is more rapid and the emergent scaling behavior is more crisp. Moreover, the kinetic Ising model considerably simplifies at zero temperature, and for the TDGL equation the simplification is even more drastic, as the governing equation turns into a *deterministic* nonlinear partial differential equation.

Recent studies of the fate of the kinetic Ising model that is quenched to zero temperature gave results that contradict the naive expectation that the system merely reaches one of the two ground states [4]–[11]. For $d \geq 3$, the kinetic Ising model gets trapped on a set of topologically complex and temporally fluctuating spongy states, so that the ground state is never reached in the thermodynamic limit [5, 6]. The topological structure of the accessible state space at long times has been found to be replete with many saddle points [12], which may explain some of the strange features of the 3d system. In $d = 2$, the kinetic Ising model reaches either ground states or states with straight stripes (all vertical or horizontal) [5, 7]. There is also a tantalizing connection between the fate of the 2d kinetic Ising model and the equilibrium critical behavior in the seemingly unrelated system of critical continuum 2d percolation [8, 9]. This percolation mapping allows one to extract apparently exact predictions for the probabilities of the 2d kinetic Ising model to freeze into the ground states or stripe states [8], and even the probabilities to reach states with inclined straight stripes (with arbitrary winding numbers in horizontal and vertical directions) that occur for the 2d TDGL equation. There are additional intriguing connections to 2d critical percolation that give exact predictions for the geometric properties of the kinetic Ising model in the coarsening regime [10].

Our main goal here is to investigate the long-time phase-ordering kinetics of systems with more than two degenerate ground states after a quench to zero temperature. There are two natural examples of such systems. The first is the q -state kinetic Potts model (with $q \geq 3$) on the square lattice, in which evolution occurs by single spin-flip dynamics. We also study a complementary continuum description that is based on the TDGL equation. The latter provides a more general description of phase-ordering kinetics because it is heavily based on symmetry considerations rather than fidelity to a particular microscopic system.

The two-dimensional q -state kinetic Potts model that is quenched to zero temperature was investigated in the 1980s, which predates many studies of the corresponding kinetic Ising model. One of reasons for this earlier focus on the Potts model is that kinetic trapping phenomena are much more pronounced [13, 14], and unusual relaxation properties [15] become evident already for small systems. Numerical work, especially simulations of quenches to positive subcritical temperatures, was additionally driven by applications, e.g., to coarsening in soap froths [16] and magnetic grains [17], and to the description of emergent structures of cellular tissues [18]. Simulations also indicated that general subcritical quenches exhibit standard coarsening for early times [19, 20]. This continuous evolution stops because the system gets trapped in a disordered state and escape from this state is slow because the process is thermally activated [21]. When the final temperature is zero, it was noticed previously that the ground state may not be reached [22, 23]. It was further suggested that for $q \geq d + 1$, glassy evolution can occur [20, 21, 24, 25] because the system gets pinned in a disordered state and the ultimate relaxation to equilibrium proceeds via thermally activated processes [20, 21], [26]–[28]. From a more geometrical perspective, recent work [29] determined the distribution of hull enclosed areas of the 2d kinetic Potts model during the coarsening regime.

With the huge increase of computing power since the 1980s, one can try to settle the fate of the 2d kinetic Potts model that is quenched to zero temperature. When

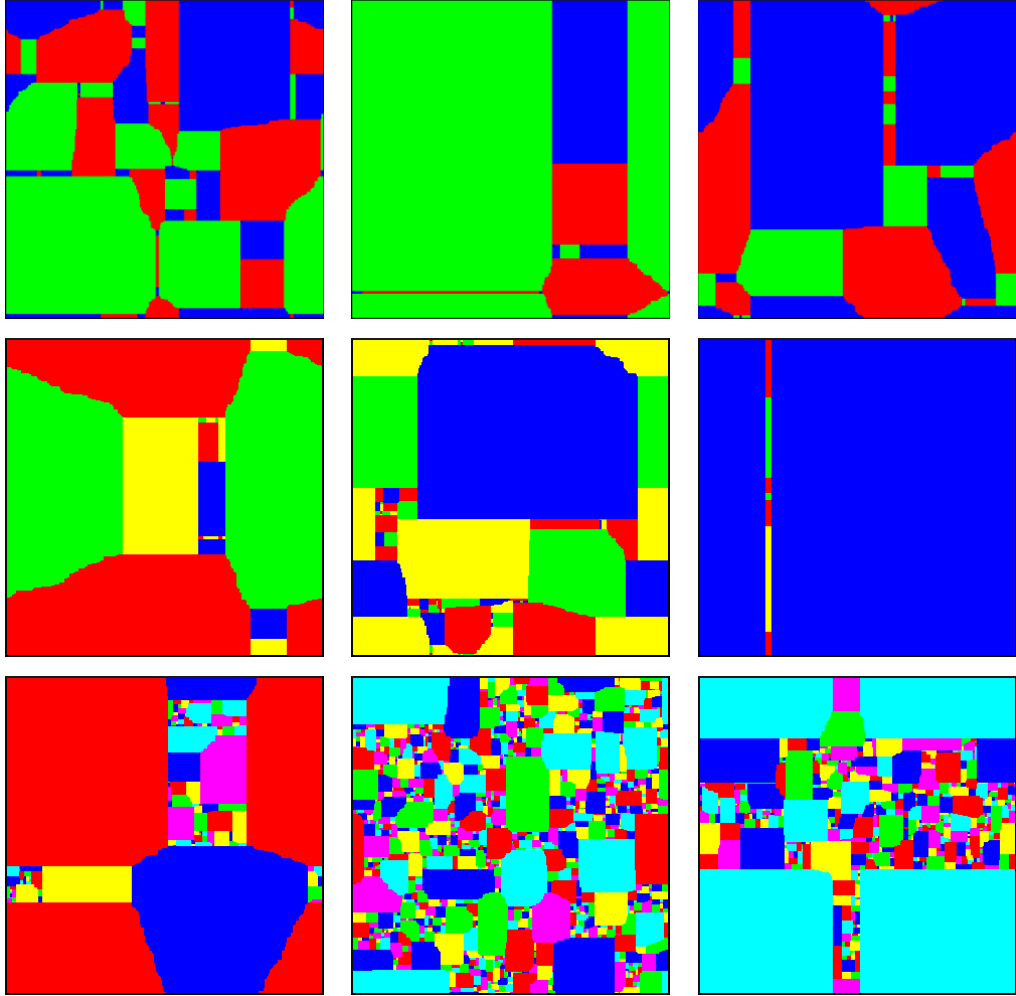


Figure 1. Representative long-time states of the 3-state (top) 4-state (middle) and 6-state (bottom row) Potts model on a square lattice of linear dimension $L = 384$ after quench from $T = \infty$ to 0. Notice that only the configuration in the middle right, with only vertical or horizontal interfaces, is static. All others, with non-straight interfaces, are still evolving, and some may evolve *ad infinitum*.

the system is sufficiently isotropic, e.g., when the underlying lattice is triangular³ the relaxation appears to be rapid [15], while on the square lattice the system can get pinned in a disordered state. We therefore limit ourselves to the most anisotropic (even-coordinated) 2d lattice, the square lattice, and we ask about the possible outcomes in the thermodynamic limit (representative long-time states are shown in figure 1). Our simulations lead to the following conclusions:

- Ground states are reached with non-zero probability.
- More complicated static states are also reached with non-zero probability.
- The system may wander *ad infinitum* on an iso-energy subspace of blinker states.

³ Similar behaviors have been observed [15] on the square lattice with additional next-nearest-neighbor ferromagnetic interactions.

The latter possibility has not been seen in earlier work, and it has come as a surprise to us. Indeed, the common lore in phase-ordering kinetics is that, in following an energy-decreasing path, the system can fall into a metastable state, not into a collection of such states. We are aware of one counterexample to the above rule, namely, the fate of the Ising model that is quenched to zero temperature, but only in greater than two dimensions⁴; in $d = 2$, static states are always reached.

The 2d kinetic Potts model undergoes an extremely slow relaxation that, in a finite fraction of realizations, is reminiscent of the 3d Ising model [6]. In the Ising case, slow relaxation is driven by rare events in which diffusively fluctuating interfaces with an additional entropic repulsive bias ultimately merge. The rarity of such coalescence events causes a logarithmically slow decay in the energy of the system. The ultra-slow evolution in the Potts model has the same origin. We shall see, however, that interface merging can sometimes lead to a rapid and drastic reordering of the global domain structure in the 2d Potts model. This avalanching is unpredictable—small stochastic fluctuations in the domain coarsening at long times can generate substantially different long-time cluster geometries.

We also emphasize that the most ‘obvious’ outcome, namely, that the 2d kinetic Potts model reaches the ground state with non-zero probability, is by no means obvious from simulations. For the 3-state Potts model, the probability to reach the ground state initially decreases as the linear dimension L of system grows and a naive extrapolation of the small- L data to $L \rightarrow \infty$ suggests that this probability vanishes in the thermodynamic limit. For larger system sizes, however, the probability starts to grow. Such a non-monotonic behavior is more clean for the kinetic Potts model with $q > 3$, leading to the conclusion that the ground state is reached with positive probability.

The second major part of our work is the study the evolution of the 2d Potts system that is based on the TDGL equation. This is a manifestly isotropic framework and the results are conceptually easier to interpret because the dynamics are not accompanied by the anomalous discreteness effects that characterize the behavior of the kinetic Potts model. Thus in the TDGL equation with three degenerate ground states, the final states are always static. However, these final states are much more rich than those that arise in the TDGL equation with two degenerate ground states (figure 2). For example, we observed states with three hexagons (in roughly 11% of realizations for $L = 128$), states with four clusters—two squares and two octagons—(roughly 8% of realizations), and six-cluster states (roughly 0.2% of all realizations). In spite of the diversity of geometrically complex states, the probability of reaching the ground state has the approximate value 0.7 for the largest systems that we simulated, and appears to remain positive in the thermodynamic limit.

Although we extensively simulate the kinetic Potts model with $q = 3, 4, 5, 6$, it is still difficult to extract reliable estimates for basic observables, such as the probability to reach a ground state, the probability to end in blinker states, etc. The reasons for this difficulty are twofold. First, the relaxation is extremely slow and many realizations are still evolving, with their ultimate fate still undecided, at times that are orders of magnitude longer than

⁴ More precisely, the probability to reach a static state is finite for the 3d kinetic Ising model on a torus, but this probability very quickly decays as the system size is increased [5, 6].

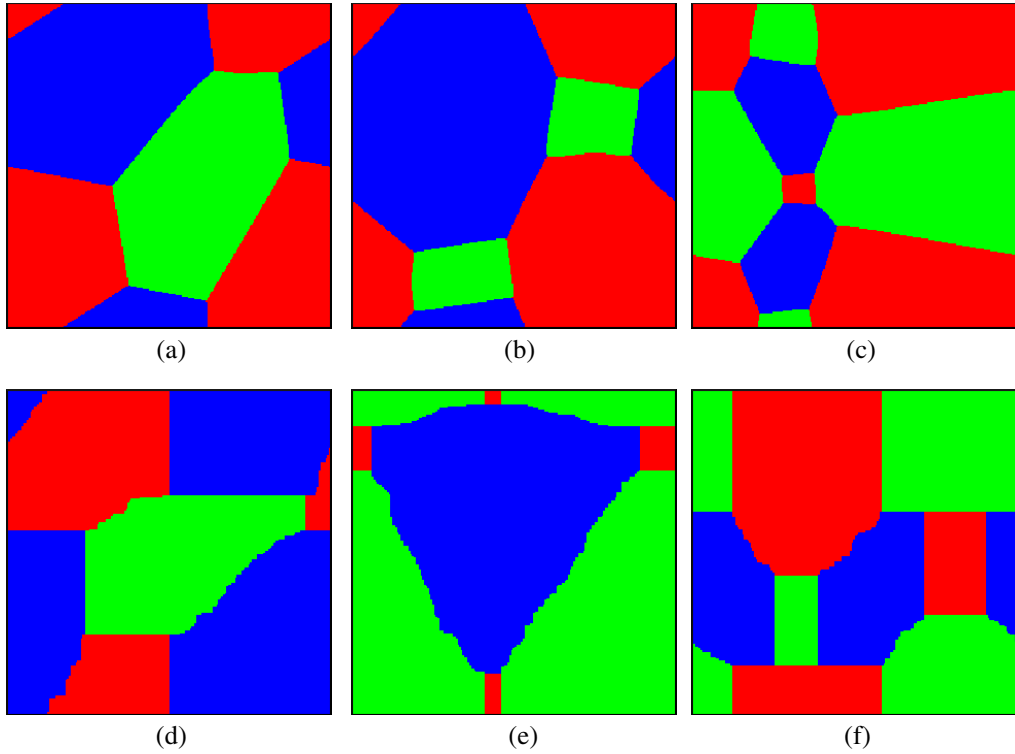


Figure 2. Long-time states from integration of the three-state TDGL equation with $L = 256$ (a)–(c) and simulations of the 3-state Potts model with $L = 192$ (d)–(f).

the coarsening time, which scales as L^2 . (The situation is more clear for $q = 3$, where one can often resolve that a system is in a genuine blinker state.) If we stop simulations at the coarsening time, the time to simulate a system of linear dimension L scales as L^4 . A second difficulty is that for the system sizes that we are able to simulate, substantial finite-size effects arise that obscure the thermodynamic behavior. Collection of all of our data took roughly ten days of computing time on a 32-CPU cluster, with each CPU running at 2 GHz.

Our simulations for the 2d kinetic Potts model with $q = 3, 4, 5, 6$ lead to the conclusion that the probabilities Π_q to reach the ground state remain positive in the thermodynamic limit:

$$\Pi_q > 0 \quad \text{for all } q \geq 2. \quad (1)$$

Even for the 2d kinetic Ising model this statement is conjectural, although in this case the connection with 2d critical continuum percolation leads to the precise conjecture [8]

$$\Pi_2 = \frac{1}{2} + \frac{\sqrt{3}}{2\pi} \ln \left(\frac{27}{16} \right) = 0.644\,24\dots, \quad (2)$$

for free boundary conditions and $\Pi_2 = 0.661\,169\dots$ for periodic boundary conditions; these are well supported heuristically and numerically [8, 9].

2. Models

2.1. Kinetic Potts model

The Hamiltonian of the Potts model is

$$\mathcal{H} = - \sum_{\langle ij \rangle} \delta(\sigma_i, \sigma_j) \quad (3)$$

where $\delta(\sigma_i, \sigma_j)$ is the Kronecker delta function, each spin σ_i takes one of the q integer values $1, 2, \dots, q$, and the sum $\langle ij \rangle$ is over all nearest-neighbor pairs. We are interested in the long-time state of the system following a quench from infinite temperature to zero temperature. Thus we initialize the lattice with equal fractions of each of the q spin states; the assumption that the initial temperature is infinite implies that the initial spin values in different sites are uncorrelated.

We employ zero-temperature Glauber dynamics [30] in which each spin-flip event that would decrease the energy occurs with rate 1, while each flip event that would conserve the energy occurs with rate 1/2. At long times, the number of flippable spins (those whose flips would conserve or decrease the energy) is small, since all evolution occurs on interfaces of large domains. For efficiency, we therefore track all flippable spins. For each such spin σ_i the corresponding flip rate R_i is determined from all of its possible transitions. Each update event then consists of selecting a flippable spin at random, flipping it, and incrementing the time by $1/(\sum_i R_i)$ [31]. After each such spin-flip event, the list of flippable spins is also updated.

Our simulations are performed on square $L \times L$ lattices with periodic boundary conditions, and our goal is to extract the results in the $L \rightarrow \infty$ thermodynamic limit. One could consider different boundary conditions, e.g., free boundary conditions, and different geometries, e.g., $L \times rL$ rectangles, and investigate the $L \rightarrow \infty$ limit, with the aspect ratio r held constant. The influences of these modifications have been investigated in the Ising case [8, 9], and these extensions have provided crucial support in favor of the connection to 2d critical continuum percolation. The boundary conditions and the aspect ratio similarly affect quantitative results in the Potts case, but for simplicity we limit ourselves to periodic boundary conditions and to square systems.

We tacitly assume (when not stated otherwise) that the densities for all q spin states are equal. In simulations of finite systems we always start with an equal number of spins of each species; thus for $q = 3$, we choose L to be divisible by 3, so that there are initially $\frac{1}{3}L^2$ spins of each type. This choice of equal initial densities for the q states is physically natural because it corresponds to an initial supercritical temperature, $T_i > T_c$. It is possible, however, to organize a disparity in the densities in each state; in the Ising case, for example, an applied external magnetic field can be turned off when the quench occurs. Our results for the general case when the initial densities in each state are unequal are briefly discussed in section 3.

2.2. Time-dependent Ginzburg–Landau (TDGL) equation

Because discrete models of kinetic spin systems are too complex to solve analytically, especially in more than one dimension, much effort has focused on phenomenological continuum models [3]. The latter are often better suited for analytical and numerical

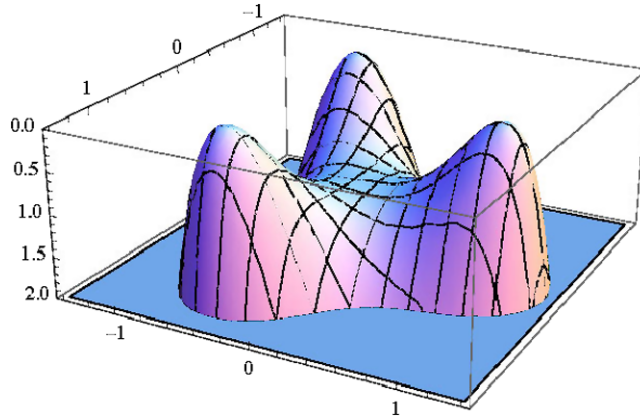


Figure 3. The negative of the potential, $-(\phi - \mathbf{A})^2(\phi - \mathbf{B})^2(\phi - \mathbf{C})^2$, which corresponds to the TDGL-equation description of the 3-state Potts model.

work; additionally, continuum models can better mimic the dynamics of real systems. For the Ising model ($q = 2$), the simplest continuum description is based on a scalar magnetization field $\phi(\mathbf{x}, t)$ and the free-energy functional

$$F_2[\phi] = \int [(\nabla\phi)^2 + (\phi - 1)^2(\phi + 1)^2] \, d\mathbf{x} \quad (4)$$

that evolves by gradient descent

$$\frac{\partial\phi}{\partial t} = -\frac{\delta F_2}{\delta\phi} = 2\nabla^2\phi + 4\phi(1 - \phi^2). \quad (5)$$

The double-well potential $V(\phi) = (\phi - 1)^2(\phi + 1)^2$ has two degenerate minima that correspond to the ground states. The field ϕ flows to one of the two potential minima, and the Laplacian term captures the effects of the surface tension between neighboring clusters. While there is no direct connection to the Ising model, this TDGL-equation description accurately describes coarsening in the Ising model and related systems [8, 9, 32].

We now formulate an analogous TDGL-equation description of non-conserved coarsening for systems with more than two degenerate ground states. For three degenerate states, we postulate the free-energy functional:

$$F_3[\phi] = \int [(\nabla\phi_1)^2 + (\nabla\phi_2)^2 + (\phi - \mathbf{A})^2(\phi - \mathbf{B})^2(\phi - \mathbf{C})^2] \, d\mathbf{x}, \quad (6)$$

with a two-component order parameter $\phi(\mathbf{x}, t) = \{\phi_1(\mathbf{x}, t), \phi_2(\mathbf{x}, t)\}$, and a potential that has three symmetrically located minima in the plane (figure 3). We may choose $\mathbf{A}, \mathbf{B}, \mathbf{C}$ to be at the corners of the equilateral triangle

$$\mathbf{A} = (1, 0), \quad \mathbf{B} = \frac{1}{2}(-1, \sqrt{3}), \quad \mathbf{C} = \frac{1}{2}(-1, -\sqrt{3}).$$

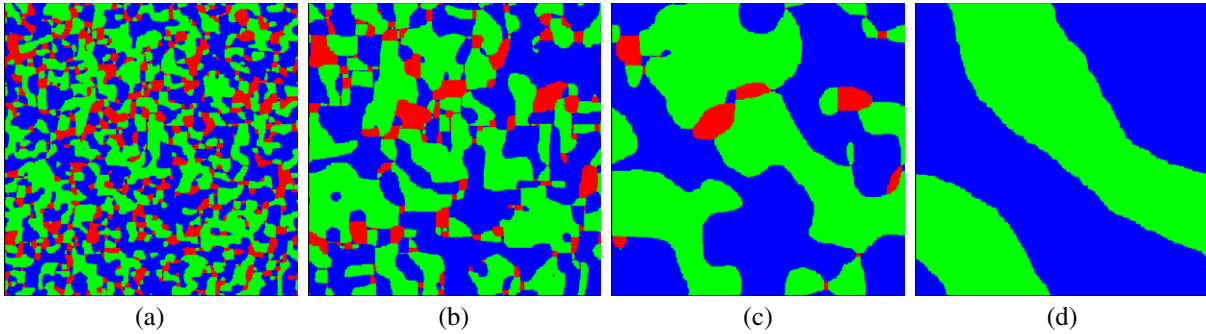


Figure 4. Coarsening of the 3-state Potts model to a diagonal stripe for linear dimension $L = 768$, with respective initial densities of red, green, and blue $\frac{10}{32}$, $\frac{11}{32}$, and $\frac{11}{32}$. See [33] for an animation of this evolution. (a) $t = 200$, (b) $t = 1000$, (c) $t = 5000$ and (d) $t = 50000$.

Gradient descent now leads to the coupled equations of motion

$$\frac{\partial \phi_1}{\partial t} = 2\nabla^2 \phi_1 - \frac{\delta}{\delta \phi_1} [(\phi - \mathbf{A})^2 (\phi - \mathbf{B})^2 (\phi - \mathbf{C})^2], \quad (7a)$$

$$\frac{\partial \phi_2}{\partial t} = 2\nabla^2 \phi_2 - \frac{\delta}{\delta \phi_2} [(\phi - \mathbf{A})^2 (\phi - \mathbf{B})^2 (\phi - \mathbf{C})^2]. \quad (7b)$$

For the continuum system, there are several natural choices for the initial condition: (i) ϕ uniformly distributed on a circle of unit radius, (ii) ϕ uniformly distributed within a ball of radius $\epsilon \ll 1$, (iii) ϕ that equiprobably takes the values \mathbf{A} , \mathbf{B} , or \mathbf{C} . We find that the long-time behavior is largely independent of the initial conditions.

3. Non-symmetric initial conditions

The initial state where the densities of the different spin states are equal is the most physically relevant as it corresponds to quenching from a supercritical temperature. The more general case is still interesting, arising, e.g., when the system was in a magnetic field before the quench. We first study what happens when not all initial densities are equal in the simplest non-trivial case of the 3-state Potts model.

There are two natural types of non-symmetric initial conditions: (i) one species in the majority, and (ii) one species in the minority, while the other two more abundant species have equal concentrations. In case (i), simulations indicate that the final outcome is always the ground state of the initial majority species. In case (ii), simulations show that the minority species disappears relatively quickly, so that the long-time dynamics is Ising like. Figure 4 shows the evolution of the 3-state Potts model on a square lattice of linear dimension $L = 768$ when the initial densities of the three states are $\frac{1}{3} + \epsilon$ (blue), $\frac{1}{3} + \epsilon$ (green), and $\frac{1}{3} - 2\epsilon$ (red), with $\epsilon = \frac{1}{96}$. The important feature is that the evolution is Ising like in the long-time limit. For this example, the two persisting species evolve into a very long-lived (1, 1) stripe topology, an event that occurs with roughly 4% probability⁵ in the kinetic Ising model [9].

⁵ In the Ising model with nearest-neighbor interactions, this (1, 1) stripe eventually disappears, but this topology is stable when second-neighbor interactions exist; see [9].

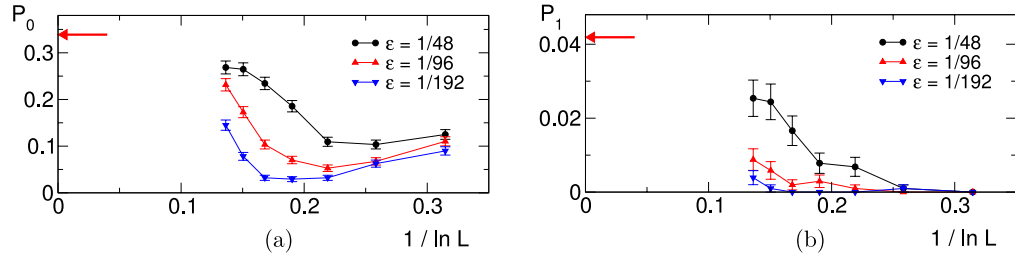


Figure 5. Probabilities of freezing into: (a) a $(1, 0)$ stripe or (b) a $(1, 1)$ stripe versus $1/\ln L$ for the 3-state Potts model for different ϵ values. The arrows indicate the theoretical predictions from the Ising model [8, 9].

As a more stringent test of whether this initial condition corresponds to the kinetic Ising model, we study the probability that the system reaches a $(1, 0)$ (equivalently $(0, 1)$) or a $(1, 1)$ stripe state when the initial densities of the three spin states are $\frac{1}{3} + \epsilon$, $\frac{1}{3} + \epsilon$, and $\frac{1}{3} - 2\epsilon$ for varying ϵ (figure 5). Here the notation (m, n) denotes a domain that winds m times around the torus in one coordinate direction and n times in the orthogonal direction. The freezing probabilities into these distinct (m, n) stripe topologies on periodic $L \times L$ lattices was previously found in the kinetic Ising model [8, 9]. For the 3-state Potts model, it appears that the probabilities of reaching the $(1, 0)$ and $(1, 1)$ stripe states are slowly approaching the Ising model predictions, even for the smallest value of $\epsilon = \frac{1}{192}$ that we studied. These results therefore suggest that dynamical behavior that is intrinsically associated with the presence of all states in the 3-state Potts model occurs only when the initial densities of the three spin states are equal. In the remainder of this paper, we will therefore concentrate on this symmetric initial condition for the general q -state Potts model.

We now briefly discuss the fate of the Potts model with arbitrary initial densities for general q . For the Ising model with initial magnetization $m_0 \neq 0$, it is believed that on an even-coordinated lattice in $d \geq 2$, the majority ground state is reached with probability one in the thermodynamic limit. In other words, the final magnetization is $m_\infty = \text{sgn}(m_0)$.⁶ This intuitively appealing property has been proved [34] only in the $d \rightarrow \infty$ limit. Thus it is still a conjecture even in two dimensions (where the connection with 2d continuum percolation [8] ‘explains’ why the majority ground state should be reached).

For the Potts model, we denote initial densities by m_1, \dots, m_q . We can always relabel the spin types to ensure that these densities satisfy $m_1 \geq m_2 \geq \dots \geq m_q$, and the normalization constraint $m_1 + \dots + m_q = 1$. Our numerical simulations (section 3) of the 3-state kinetic Potts model indicate three possibilities:

- (i) $m_1 > m_2 \geq m_3$. The majority ground state is reached.
- (ii) $m_1 = m_2 > m_3$. The fate of this 3-state kinetic Potts model is the same as that in the Ising model: the minority phase disappears, and the system either reaches the ground state of one of the two majority phases (which occurs with probability equation (2)), or a stripe state with stripes composed of spins of the majority phases is reached (which occurs with the complementary probability $1 - \Pi_2$).

⁶ The one-dimensional case is exceptional, both ground states can be reached, e.g., the plus ground state is reached with probability $(1 + m_0)/2$.

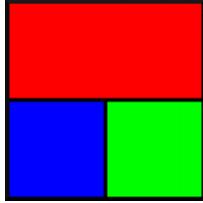


Figure 6. A T-junction in the 3-state Potts model.

- (iii) $m_1 = m_2 = m_3$. This is the only point where the fate of the system is novel, and it faithfully represents the 3-state Potts model.

Based on the above findings, we conjecture that the q -state Potts model with initial densities $m_1 = \dots = m_Q > m_{Q+1} \geq \dots \geq m_q$ exhibits the same behavior as the Q -state Potts model with equal initial densities. It is feasible that this conjecture is actually valid not only on the square lattice, but for other (even-coordinated) lattices of arbitrary spatial dimension $d \geq 2$.

4. Cluster geometry at long time

4.1. Kinetic Potts model

For the kinetic Potts model, fundamental questions that we investigate are: (i) what is the nature of the long-time state? Is the ground state eventually reached or is there freezing into more complex final states? (ii) What is the time dependence of the long-time relaxation? The examples in figure 1 suggest that the ground state is likely not reached, but rather the final state typically consists of a domain mosaic with characteristic length scale L and with ‘breathing’ domain walls; such states are the analogs of blinker states that arise in quenches of the 3d Ising model to zero temperature. Our simulations indicate, however, that this outcome is just one of the three possibilities mentioned in section 1. Namely, in the thermodynamic limit the system falls into a ground state, or a more complicated static state, or it wanders on a set of equal-energy blinker states (see also [22]). As already mentioned in section 1, it is hard to provide quantitative predictions for these probabilities (see also section 5).

For the 3-state Potts model, the fundamental reason for the increased cluster complexity compared to the Ising model is that an interface between domains may have a beginning and an end. The termini of these interfaces occur at T-junctions where three distinct spin states appear in the elemental plaquette that circumscribes the junction (figure 6). Each of these spins has at least 2 neighbors in the same state and thus cannot flip at zero temperature; the importance of these T-junctions was first noted in [15, 22]. These T-junctions therefore pin domain boundaries and provide a multitude of ways for the 3-state Potts model to get stuck in an infinitely long-lived metastable state (at zero temperature), such as the examples on the top line of figure 1. For larger q , more complex interface junctions can arise, which suggest that pinning of domain walls is even more likely to occur.

To understand the long-time state of the q -state Potts model, consider the time dependence of the energy for q between 3 and 6 (figure 7). At early times, the energy

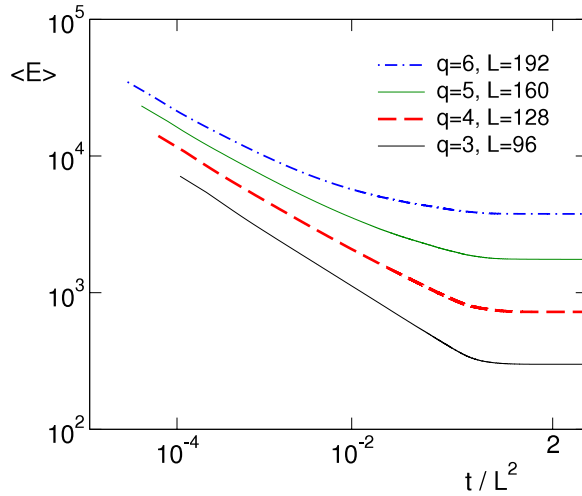


Figure 7. Average energy versus t/L^2 for the q -state Potts model for $q = 3$ –6. The average is over 4096 realizations for $q = 3$ and 512 realizations for larger q .

decays in a manner that is consistent with a power-law time dependence, as expected from curvature-driven coarsening [2, 35]. This apparent power-law decay defines the coarsening regime. By time $t \approx L^2$, the decrease in the energy has essentially stopped, although we shall see that there are subtle relaxation mechanisms that arise at much longer times. For both tractability and concreteness, most of our observations are based on measurements at time $\tau_c = 2L^2$, which we define here as the Potts coarsening time. We choose this value of τ_c because it is safely beyond the initial coarsening regime, so that a typical realization of the system is pinned in a quasi-final state.

We now focus on the systematic q dependences of basic observables in the q -state Potts model at $\tau_c = 2L^2$ (figure 8). Perhaps the most surprising feature is the behavior of the probability Π_q to reach the ground state in the limit of $L \rightarrow \infty$. For all $q \geq 3$, Π_q varies non-monotonically with L , and the data suggest that the probability of reaching the ground state will be greater than zero as $L \rightarrow \infty$ for any $q \geq 3$. It is paradoxical that as the number of Potts states is increased, the data also suggest that it is more likely that a finite system will reach the ground state (figure 8(a)). We will provide more details about this intriguing phenomenon below.

Next, we consider the L dependence of the energy per spin. If one fits these data to a power law (which becomes more dubious for larger q), this normalized energy decays roughly as $L^{-0.8}$ for $q = 3$, and progressively more slowly with L for larger q . As one might naively anticipate, as the number of Potts states increases, a typical realization at the coarsening time consists of progressively smaller patches of single spin states. Concomitantly, there would be more interfaces for larger q and the normalized energy should therefore decay progressively more slowly with L .

Finally, let us examine the average number of clusters N_c . Strictly speaking, we cannot cleanly probe N_c for sufficiently large L , as the true asymptotic regime is beyond the reach of the simulations for many realizations. Nevertheless, we can still infer some basic q -dependent properties: for $q = 6$, the average number of clusters grows roughly as L^2 . This result indicates that for $q = 6$ (and larger), domains typically have a size comparable to the lattice spacing, so that their number grows linearly with the area of the system.

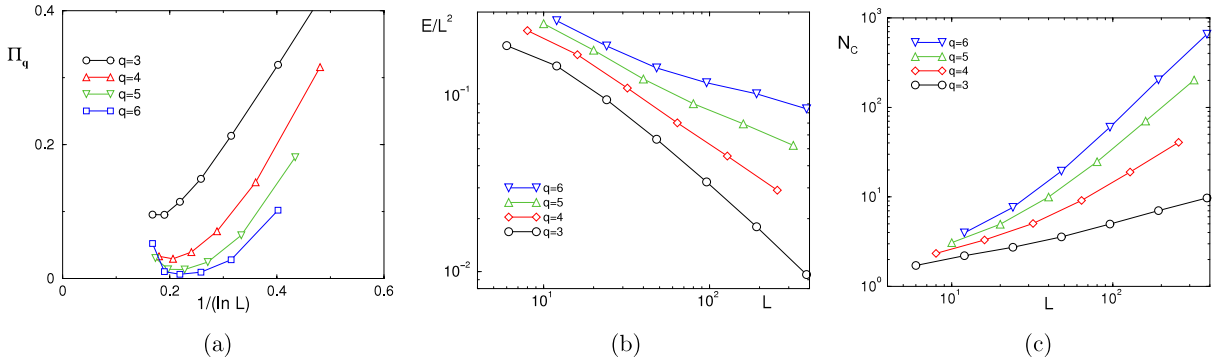


Figure 8. (a) Probability Π_q for the q -state Potts model to reach the ground state by time $2L^2$ following a quench to zero temperature. The data for the largest two values of L for $q = 3$ and for the largest value of L for $q = 4, 5, 6$ are based on 2^{14} realizations; all other data are based on 2^{17} realizations. Error bars are smaller than the size of the symbols. (b) Average energy per spin and (c) average number of clusters versus L for the q -state Potts model with $q = 3-6$.

In contrast, for $q < 6$, N_c grows more slowly than L^2 , indicating that in these cases a characteristic domain length increases with system size.

Interestingly, as the number of spin states q increases, the probability to reach the ground state Π_q becomes more likely, while the average number of clusters N_c grows more rapidly with L . These seemingly incompatible behaviors are not necessarily contradictory, however. Even if it becomes more likely to end up with a single cluster (the ground state) for larger q , the *average* number of clusters can still grow linearly in the area of the system. Importantly, this growth rate increases with q .

4.2. TDGL equation

For the case of three degenerate ground states, we start with $\phi(x, y, t)$ in one of the symmetric and disordered initial configurations (i)–(iii) given in section 2.2 and numerically integrate the TDGL equations (7) in time on $L \times L$ lattices, with $L = 16, 32, 64, 128$. We stop the integration at time $t = L^2$, which is at the end of the coarsening regime for the 3-state TDGL. Figure 2 (top) shows three non-trivial outcomes from these integrations. To make this plot, we map the continuous order parameter in the TDGL equation to one of three discrete values that depend on whether ϕ lies inside the wedge with angular range $(\pi/3, -\pi/3)$ that is centered on the potential minimum at $\mathbf{A} = (1, 0)$, the wedge $(\pi/3, \pi)$ that is centered on $\mathbf{B} = \frac{1}{2}(-1, \sqrt{3})$, or the wedge $(-\pi, 5\pi/3)$ that is centered on $\mathbf{C} = -\frac{1}{2}(1, \sqrt{3})$. After this discretization, we identify the resulting clusters by the multi-labeling method [36].

We find that the 3-state TDGL can become trapped in unexpected types of pinned metastable arrangements, as shown in figure 2. The outcome of three hexagons (figure 2(a)) occurs in roughly 11% of all realizations, four pinned clusters (figure 2(b)) occur in roughly 8% of realizations, while a state that contains six hexagonal clusters (figure 2(c)) occurs in less than 1% of all realizations. In addition, the probability that the system gets stuck in a state that consists of two straight stripes (as in the TDGL with two ground states) occurs roughly 10% of the time, while roughly 70% of the time the ground state is reached. The

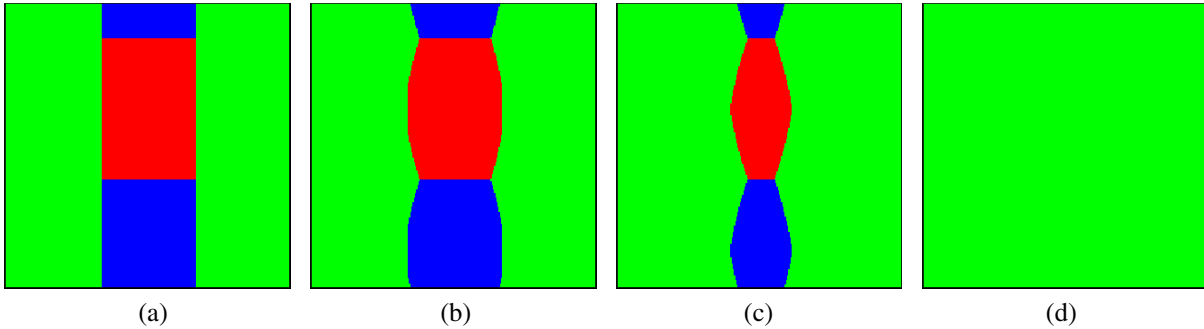


Figure 9. A multi-state stripe is stable in the discrete Potts model (a) but is unstable under TDGL evolution ((b)–(c)). The times in the plot are: (a) $t = 0$, (b) $t = 1000$, (c) $t = 7000$ and (d) $t = 12000$.

probabilities of reaching these different long-time states do depend on the system size, but the data clearly indicate that in the thermodynamic limit the probability of reaching the ground state is less than 1, while the probabilities of reaching 3- and 4-cluster states are both greater than zero.

Finally, it is worth noting an important difference between the discrete 3-state Potts model and the TDGL equation with three degenerate minima, which has consequences for the nature of the final states. In the 3-state Potts model, T-vertices that pin domain walls always contain right angles. However, the TDGL equations are isotropic, so neighboring clusters must meet at 120° angles for the 3-state model. This difference has profound implications on the cluster structure at long times. Consider the stripe state shown in figure 9(a). This configuration is stable in the Potts model, but is unstable in 3-state TDGL. Starting with this state and integrating the TDGL equations (7), the angles between domain walls at the T-junctions begin to equalize. In so doing, curvature is generated on the interface that tends to shrink the stripe and the final outcome is the ground state (figure 9(d)).

5. Ultra-slow evolution

The long-time states of the Potts system are often *not* static, but are either very long-lived or infinitely long-lived ‘blinker’ states. A blinker spin is one that can freely flip between various states without any energy cost, and a blinker state is a configuration that contains multiple blinker spins. These blinker states also arise in zero-temperature quenches of the 3d kinetic Ising model; however, in the 2d Potts system, they are more readily visualized. A typical example is shown in figure 10. Here, the T-junctions are frozen in place at zero temperature, but the spins on the interfaces that connect two T-junctions can flip freely with zero energy cost.

A crucial feature of these blinkers is that they predominantly remain in their intermediate states, as in figure 10(a). This behavior arises because there exists an effective bias in the diffusive motion of the staircase interface that pushes it to an intermediate state (figure 11). In figure 11(b), there are four red and three green blinker spins, so that the red interface tends to recede. Similarly, in figure 11(c), there are four green and

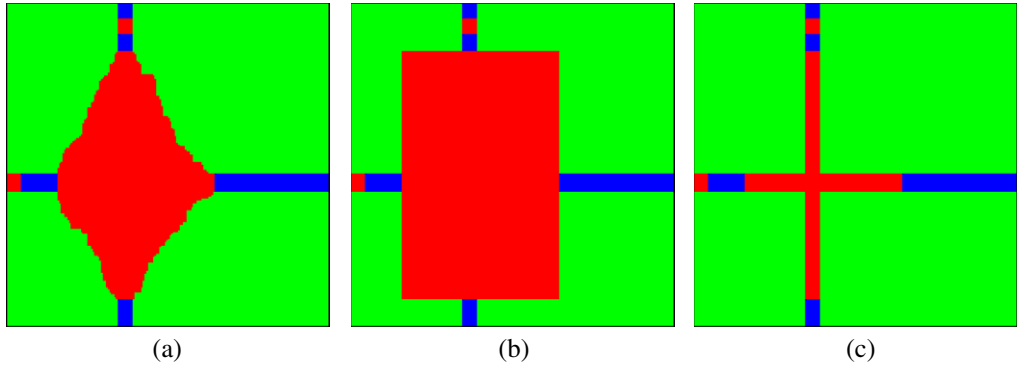


Figure 10. (a) A blinker state, with four staircase interfaces of blinker spins. The extremes where these interfaces are fully inflated (corresponding to the convex envelope of the domain in (a)) or fully deflated are shown in (b) and (c), respectively.

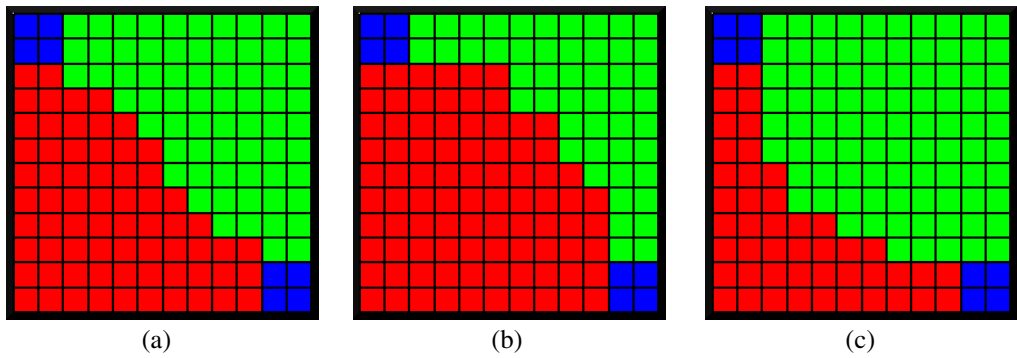


Figure 11. A staircase interface with blinker spins at the interface corners, showing the (a) intermediate, (b) partially inflated, and (c) partially deflated states.

three red blinker spins, so that the green interface tends to recede. These biases push the interface to the intermediate state, as in figures 10(a) and 11(a).

This bias towards intermediate states has profound implications for the long-time relaxation. While a single isolated interface in a blinker state can never decrease the energy of the system, interactions between two such interfaces can give rise to energy-decreasing spin flips at long times (figure 12). Here, each of the two separated blinker interfaces tends to fluctuate around their respective intermediate states. However, a rare event can occur in which these two interfaces touch, leading to irreversible energy-lowering spin flips that culminate in the red domain (northeast) and the green domain (southwest) filling their convex envelopes. The time required for this interface merging scales exponentially in the length of the domain interface [6], leading to slow relaxation. We term configurations that consist of two blinker interfaces that eventually merge at long times as *pseudo-blinkers*.

To characterize the slow relaxation, which we argue originates with pseudo-blinkers, we study the survival probability $S(t)$, the probability that there are no possible energy-lowering spin flips remaining in the system at time t after the quench. This quantity is not easy to determine because the evolution at long times is characterized by increasingly long

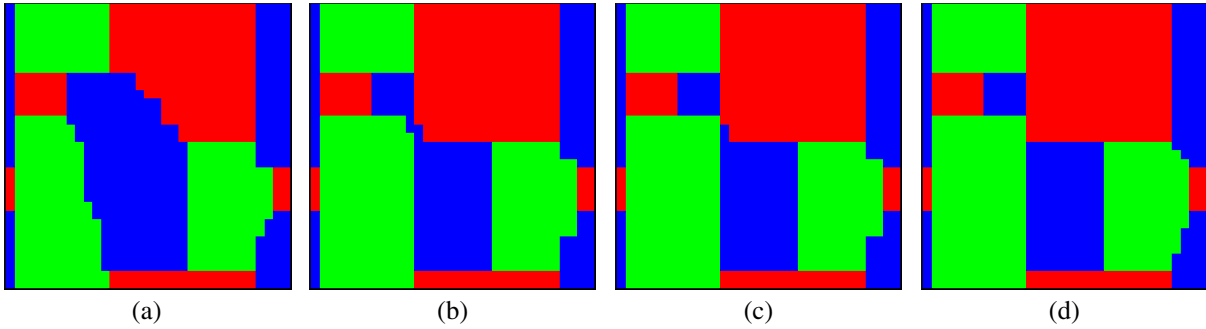


Figure 12. Interface merging in the 3-state Potts model on a 33×33 square. (a) Pseudo-blinker state with energy $E = 188$, which is first reached at $t = 251$. (b) System at $t = 16\,160\,676.9$ and (c) $t = 16\,160\,677.0$, where the blinker interfaces first touch. (d) At $t = 16\,160\,677.7$, the merging is complete and the energy is $E = 185$. See [33] for an animation of this evolution.

periods of stasis that are punctuated by very infrequent energy-lowering events (figure 12). Because a direct measurement of $S(t)$ is prohibitively time consuming, we ‘look ahead’ in the simulation to determine whether an energy-lowering spin flip could occur sometime in the distant future for a configuration that contains multiple blinker spins. Our algorithm is similar to that used to determine the survival probability in the 3d kinetic Ising model [6] and is the following.

- (i) Maintain lists of spins for which energy-lowering and energy-conserving flips may occur at the current update, \mathcal{L}_- and \mathcal{L}_0 , respectively. When \mathcal{L}_- becomes empty while \mathcal{L}_0 is non-empty, then the system may either:
 - (a) be in its lowest-energy state and wander *ad infinitum* on this iso-energy set;
 - (b) be in a finite-lifetime metastable state and a lower-energy state is reached when two blinker interfaces merge (as in figure 12).
- (ii) When \mathcal{L}_- first becomes empty while \mathcal{L}_0 remains non-empty, the configuration \mathcal{C}_0 and time \mathcal{T}_0 are saved.
- (iii) Starting from \mathcal{C}_0 , an infinitesimal magnetic field is imposed in the -1 direction:

$$\mathcal{H} = \epsilon \sum_i \delta(\sigma_i, 1) - \sum_{\langle ij \rangle} \delta(\sigma_i, \sigma_j) \quad \epsilon \ll 1. \quad (8)$$

This Hamiltonian drives the state-space motion along the iso-energy surface by forcing blinker spins in state 1 to change to either state 2 or 3. If an energy-lowering move occurs during this driving, then the system is not in its lowest-energy state. The system is returned to state \mathcal{C}_0 and is evolved with unbiased Glauber dynamics from time \mathcal{T}_0 until the next energy-lowering move occurs and then step (ii) is repeated.

- (iv) If an energy-lowering spin flip does not occur in step (iii), then this step is repeated with a field applied in the -2 direction and then in the -3 direction. If the energy does not decrease after application of all three fields, then \mathcal{C}_0 is the lowest-energy state of the system and its survival time is \mathcal{T}_0 .

Figure 13 shows the time dependence of the survival probability for the 3-state and 6-state Potts model. There are several intriguing and yet-to-be-explained features in these

Zero-temperature coarsening in the 2d Potts model

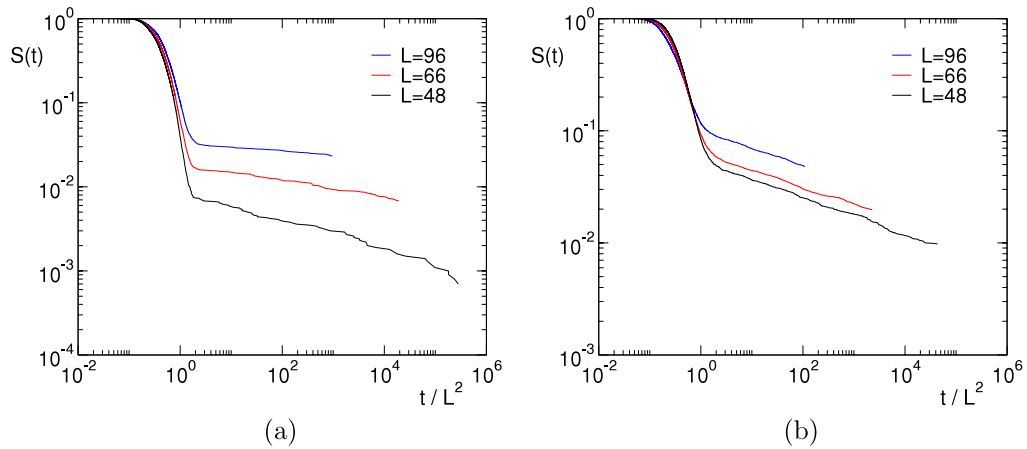


Figure 13. Time dependence of the survival probability $S(t)$, defined as the probability that the q -state Potts system has not yet reached a fixed-energy configuration. The data are based on 10^4 realizations. (a) $q = 3$ and (b) $q = 6$.

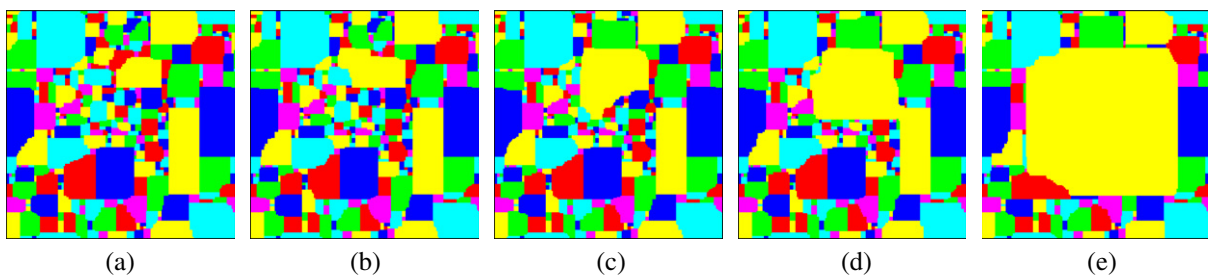


Figure 14. Cluster avalanche in the 6-state Potts model on a lattice of linear dimension $L = 192$. See [33] for an animation of this evolution. (a) $t = 630\,000$, (b) $t = 633\,000$, (c) $t = 633\,500$, (d) $t = 634\,500$ and (e) $t = 640\,000$.

plots. First, in the early-time coarsening regime, $S(t)$ shows good but not excellent data collapse when the time is rescaled by the coarsening time. Better collapse arises for the early-time 3-state Potts data when the time is rescaled by L^z , with $z \approx 2.3$. For the 6-state Potts model, the small deviation from data collapse cannot be removed by using a value for z that is different than 2. Second, relaxation at extraordinarily long times can occur. For example, for $q = 3$ and $L = 48$, there are energy-lowering spin-flip events a factor 10^5 beyond the coarsening time!

6. Avalanche dynamics for large q

For $q = 3$ pseudo-blinkers are mostly benign, as configurations that contain pseudo-blinkers typically will undergo several isolated but small decreases in energy at long times and then get trapped in either a frozen state or a true blinker state. For larger q , however, macroscopic cluster rearrangements, or ‘avalanches’, can occur, in which clusters can fill their convex envelopes, leading to successive cluster mergings (figure 14). We shall argue that the mechanism driving cluster avalanches in the Potts model for large q is an enhanced version of this filling out of the convex cluster envelopes.

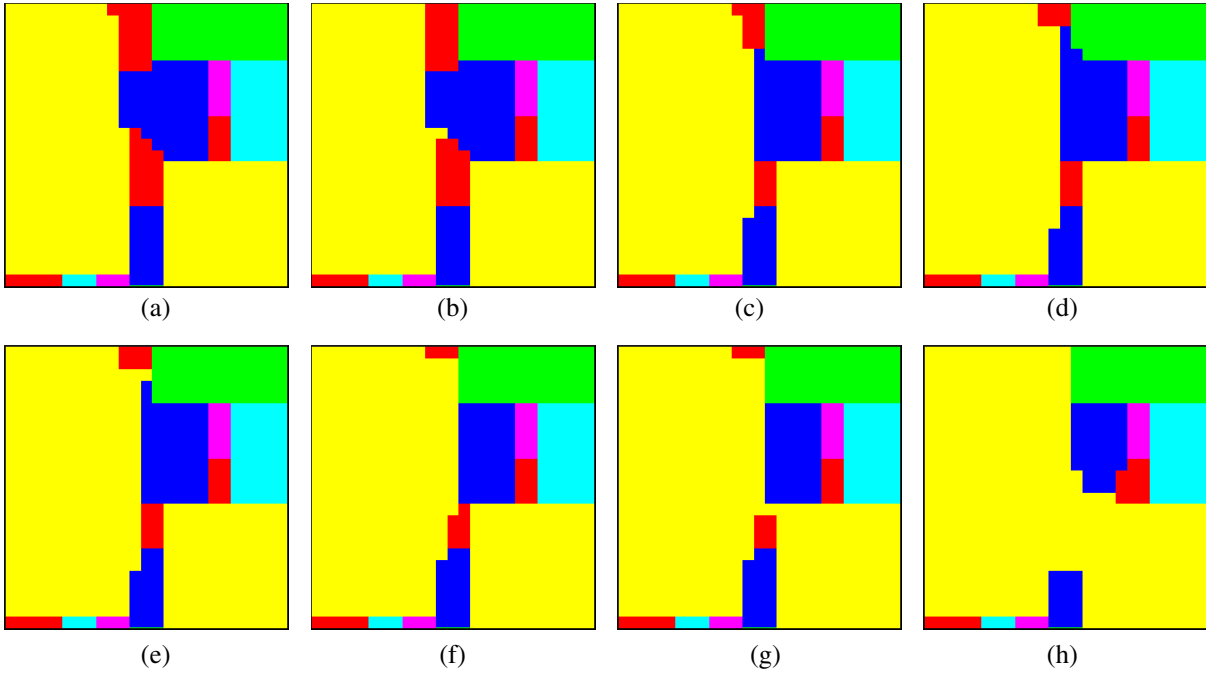


Figure 15. A zoom of figure 14 showing the event sequence that merges the two large yellow clusters in figure 14(c). In (b) and in (e), the convex envelope of the yellow cluster moves one unit to the right. In (g), a single spin flip merges the two yellow clusters. The times in the plots are: (a) $t = 634\,396.5$, (b) $t = 634\,396.8$, (c) $t = 634\,455.0$, (d) $t = 634\,459.4$, (e) $t = 634\,459.7$, (f) $t = 634\,471.5$, (g) $t = 634\,471.7$ and (h) $t = 634\,490.0$.

Figure 14 shows a typical avalanche in the 6-state Potts model. In (b), two small yellow clusters merge and this composite cluster begins to fill its convex envelope. The resulting cluster continues to grow by additional mergings and convex envelope filling (c), and then merges with a large cluster to the southeast (d). The merged cluster ultimately fills its convex envelope at $t = 640\,000$, where the lowest-energy state has been reached (e). The avalanche occurs at $t \approx 633\,000$, which is an order of magnitude greater than the coarsening time. This avalanche also leads to a macroscopic decrease of nearly 50% in the energy—from 5051 to 2849!

However, if the filling of convex envelopes is the driving mechanism for avalanches, then the system would never evolve from figure 14(c) to (d) because the convex envelopes of the two large yellow clusters in figure 14(c) do not overlap. These two clusters do merge because spin-flip events occur that allow a single cluster to expand beyond its convex envelope. The sequence of events that illustrate this domain expansion and subsequent cluster merging are shown in figure 15. The microscopic events that underlie this expansion are illustrated in figure 16. When the number of spin states is three or greater, then spin-flip events allow a protrusion to form on a straight domain boundary. This protrusion can grow and ultimately cause a straight boundary to translate by one lattice spacing laterally. When the number of spin states is greater than or equal to the lattice coordination number, then there can be spins on domain boundaries that can flip freely to *any* state, which facilitates the process of domain expansion.

3 2 2 2 2 2	3 2 2 2 2 2	3 2 2 2 2 2	3 2 2 2 2 2
3 2 2 2 2 2	3 2 2 2 2 2	3 2 2 2 2 2	3 2 2 2 2 2
3 2 3 3 3 3	3 1 3 3 3 3	3 1 1 3 3 3	3 1 1 1 3 3
1 1 1 1 1 1	1 1 1 1 1 1	1 1 1 1 1 1	1 1 1 1 1 1

Figure 16. Illustration of spin-flip events that allow a protrusion of spins in the 1 state to form and grow, ultimately leading to the lateral translation of a straight interface.

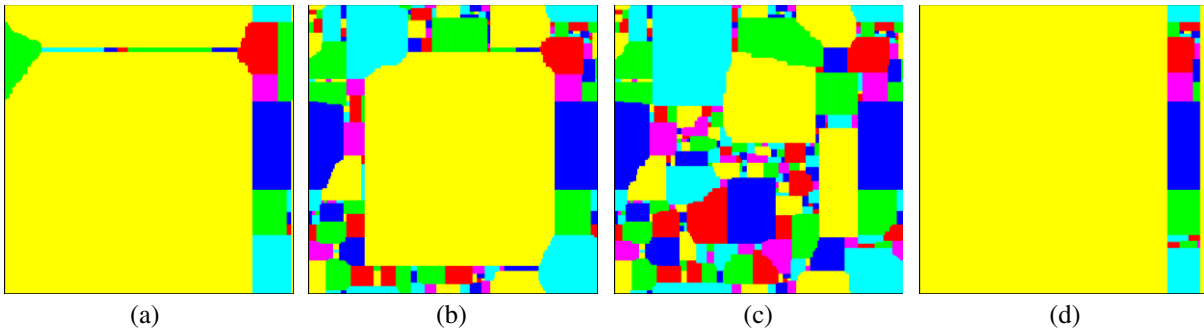


Figure 17. Four long-time states when starting with the configuration of figure 14(b).

These long-time avalanches also evolve unpredictably. To illustrate this point, we started with the configuration in figure 14(b) (immediately after the two pseudo-blinkers merge) and we simulated 10^4 independent realizations of the dynamics. The final state energies of this subset of realizations range between $E = 490$ and 4383 , with $\langle E \rangle = 2827$. Four representative such final states, with final energies $E = 938$, 2547 , 4103 , and 664 ((a)–(d)) are shown in figure 17. The salient point is that avalanching involves an unpredictable sequence of events, so that it is not possible to infer the final state even quite late in the evolution.

Finally, we also find the striking feature that in a small fraction of all realizations (e.g., with probability approximately 5% for $q = 6$ and $L = 384$) these avalanches can continue to completion, so that the system ultimately reaches the ground state (figure 18). In this subset of realizations, expansion of clusters to fill their convex envelopes leads to merging of clusters and a cascading sequence of merging and growth that terminates when the ground state is reached. It is striking that these macroscopic avalanches become more common as the number of Potts states is increased and that there exist both realizations that reach the ground state and realizations that get stuck in states where the typical cluster size is quite small.

7. Discussion

We studied the following basic problem: how does a system with many equivalent ground states evolve when suddenly quenched from a disordered state to zero temperature, and what are the properties of the long-time states? In the simpler case of the kinetic Ising model, the ground state is only sometimes reached in $d = 2$ and is never reached for $d \geq 3$. The feature that prevents the ground state from being reached in the three-dimensional

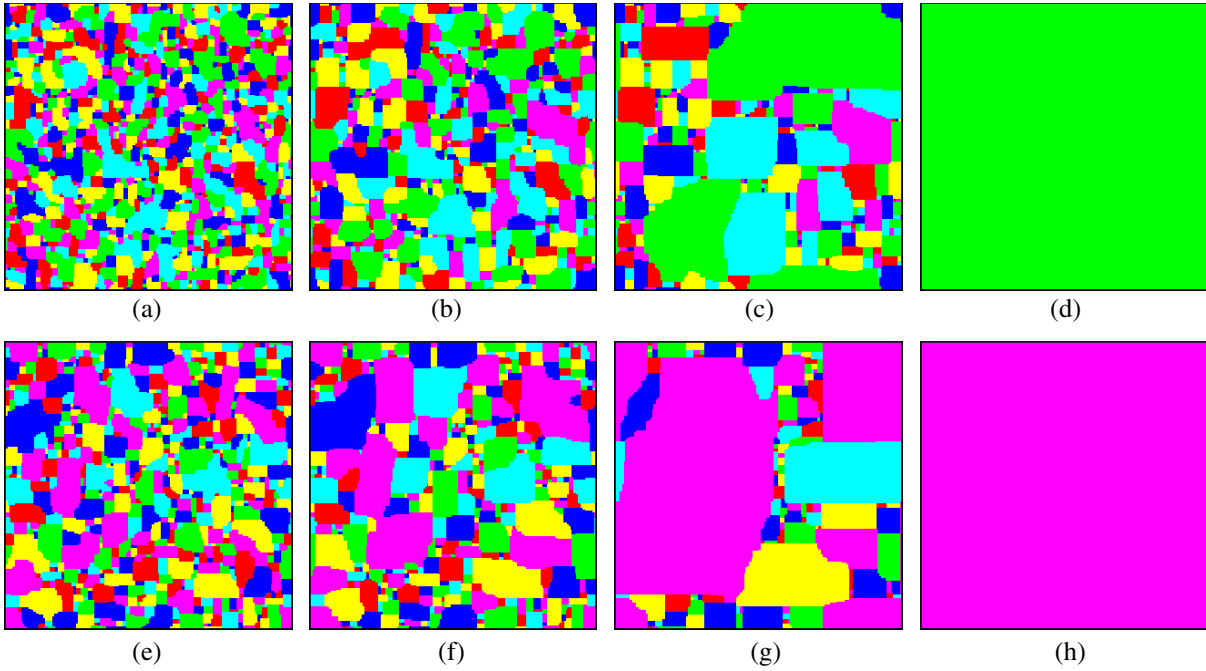


Figure 18. Two examples of a 6-state Potts model on a square lattice of linear dimension $L = 192$, with equal initial densities of the six states, that rapidly evolve to one of the ground states. See [33] for an animation of this evolution in the top line. (a) $t = 30$, (b) $t = 100$, (c) $t = 1000$, (d) $t = 7694$, (e) $t = 100$, (f) $t = 330$, (g) $t = 1000$ and (h) $t = 6784$.

Ising case is that the initial state consists of two highly intertwined spin-up and spin-down domains that cannot disentangle by local spin-flip dynamics. Partly because of this entanglement of domains in the initial state, the evolution is anomalously slow, with the characteristic timescale varying exponentially in the system size.

In this work, we extended the consideration of this basic question to the fate of the 2d kinetic q -state Potts model that is initially in a disordered state and is suddenly quenched to zero temperature. A new feature of the Potts model with $q \geq 3$ is that domain boundaries no longer have to be closed loops. Instead, boundaries can have endpoints, so that three or more boundaries can meet at a single junction. These junctions act as pinning centers that promote freezing of domains. This effect is readily apparent in the 3-state Potts model and becomes more prominent as the number of states q increases (figure 1). Thus one might expect that increasing the number of Potts states q would make it more difficult for a system to reach the ground state after a quench to zero temperature. Paradoxically, the opposite appears to be the case.

Thus one of our main results is that the Potts model reaches one of its q ground states with a non-zero probability in the thermodynamic limit. The mechanism that causes this increased likelihood for reaching the ground state is the repeated processes of: (i) clusters growing to fill their convex envelope and (ii) cluster coalescences that lead to sudden increases in the convex envelopes of the merged cluster. The combined effect of these processes can drive an avalanche in which a single expanding cluster engulfs the entire system so that one of the q ground states is reached. When the number of Potts states is

large, cluster growth is enhanced by the existence of spins on the cluster boundary that can flip freely to any spin state and thereby allow a cluster to grow beyond its convex envelope.

There are additional subtleties in Potts model coarsening. Perhaps most prominent is the existence of non-static blinker interfaces that comprise diagonal (non-vertical or non-horizontal) domain boundaries. These blinker interfaces can evolve forever without energy cost. The slow relaxation observed in the q -state Potts model arises because of the merging of two of these wandering diagonal interfaces. The timescale for these energy-lowering merging events grows exponentially with the typical domain size.

To test the universality of our results, we additionally studied a continuum system, namely the time-dependent Ginzburg–Landau (TDGL) equation, with a symmetric 3-well potential to mimic the 3-state Potts model. The resulting equations for the evolution of the order parameter are simpler and more fundamental than the myriad of microscopic models for describing coarsening of a multi-state discrete spin model. While many of our results from integration of the TDGL equations mirror those found for the discrete Potts models, the former also give rise to unexpected cluster patterns at long times that, with the benefit of hindsight, resemble the global structure of domain mosaics in the Potts model at long times. For the TDGL system with three degenerate ground states, the ground state is reached in a somewhat larger fraction of realizations than for the 3-state kinetic Potts model, but we also found more exotic static states, such as three hexagonal domains, two squares and two octagonal domains, and even a state that consists of six hexagonal domains.

The long-time coarsening of the kinetic Potts model and the multi-state TDGL equations poses many open questions that are ripe for future exploration. For instance, on the triangular lattice, the domain structure that emerges in the coarsening regime of the q -state kinetic Potts model is quite different from the corresponding domain structure on the square lattice [15], namely the lattice effects are strongly suppressed on the triangular lattice. Thus the kinetic Potts model on the triangular lattice is closer to the TDGL equation, which is isotropic. Therefore even universality with respect to lattice structure is questionable for the kinetic Potts model. In particular, it will be interesting to understand if the probability to reach blinker states remains positive (in the thermodynamic limit).

Our results for TDGL coarsening are much less extensive than for the Potts model but also suggest intriguing features, such as the existence of stable multi-cluster states, in addition to the ground state and stripe states. It would be also worthwhile to investigate the TDGL equations with q degenerate ground states. This would involve considering an order parameter in $q - 1$ dimensions with a potential that has minima at the q -vertices of a simplex. While the correspondence between the discrete spin system and the TDGL-equation results is quite close for the case of two degenerate states (the Ising model), the precise nature of the correspondence when the number of degenerate states is three or larger is still to be determined.

Acknowledgments

We thank Gary Grest and Alberto Petri for useful comments and suggestions. JO and SR gratefully acknowledge NSF Grant No. DMR-1205797 for partial financial support of this work.

References

- [1] Gunton J D, San Miguel M and Sahni P S, 1983 *Phase Transitions and Critical Phenomena* vol 8, ed C Domb and J L Lebowitz (New York: Academic)
- [2] Bray A J, 1994 *Adv. Phys.* **43** 357
- [3] Krapivsky P L, Redner S and Ben-Naim E, 2010 *A Kinetic View of Statistical Physics* (Cambridge: Cambridge University Press)
- [4] Lipowski A, 1999 *Physica A* **268** 6
- [5] Spirin V, Krapivsky P L and Redner S, 2001 *Phys. Rev. E* **63** 036118
- [6] Spirin V, Krapivsky P L and Redner S, 2002 *Phys. Rev. E* **65** 016119
- [7] Olejarz J, Krapivsky P L and Redner S, 2011 *Phys. Rev. E* **83** 030104
- [8] Olejarz J, Krapivsky P L and Redner S, 2011 *Phys. Rev. E* **83** 051104
- [9] de Oliveira P M C, Newman C M, Sidoravicious V and Stein D L, 2006 *J. Phys. A: Math. Gen.* **39** 6841
- [10] Barros K, Krapivsky P L and Redner S, 2009 *Phys. Rev. E* **80** 040101
- [11] Olejarz J, Krapivsky P L and Redner S, 2012 *Phys. Rev. Lett.* **109** 195702
- [12] Aizenberg J J, Bray A J, Cugliandolo L F and Sicilia A, 2007 *Phys. Rev. Lett.* **98** 145701
- [13] Sicilia A, Aizenberg J J, Bray A J and Cugliandolo L F, 2007 *Phys. Rev. E* **76** 061116
- [14] Blanchard T and Picco M, 2013 arXiv:1304.6758
- [15] Kurchan J and Laloux L, 1996 *J. Phys. A: Math. Gen.* **29** 1929
- [16] Safran S A, Sahni P S and Grest G S, 1982 *Phys. Rev. B* **26** 466
- [17] Safran S A, Sahni P S and Grest G S, 1983 *Phys. Rev. B* **28** 2693
- [18] Sahni P S, Srolovitz D J, Grest G S, Anderson M P and Safran S A, 1983 *Phys. Rev. B* **28** 2705
- [19] Glazier J, Anderson M and Grest G, 1990 *Phil. Mag. B* **62** 615
- [20] Thomas G L, de Almeida R M C and Graner F, 2006 *Phys. Rev. E* **74** 021407
- [21] Weaire D and Rivier N, 2009 *Contemp. Phys.* **50** 199
- [22] Raabe D, 2000 *Acta Mater.* **48** 1617
- [23] Yu Q, Nosonovsky M and Esche S K, 2008 *J. Comput. Methods Sci. Eng.* **8** 227
- [24] Zöllner D, 2011 *Comput. Mater. Sci.* **50** 2712
- [25] Srolovitz D J, Anderson M P, Sahni P S and Grest G, 1984 *Acta Metall.* **32** 793
- [26] Mombach J C M, Vasconcellos M A Z and de Almeida R M C, 1990 *J. Phys. D: Appl. Phys.* **23** 600
- [27] Grest G S, Anderson M P and Srolovitz D J, 1988 *Phys. Rev. B* **38** 4752
- [28] Ferrero E E and Cannas S A, 2007 *Phys. Rev. E* **76** 031108
- [29] de Oliveira M J, 2009 *Comput. Phys. Commun.* **180** 480
- [30] de Oliveira M J and Petri A, 2002 *Phil. Mag. B* **82** 617
- [31] de Oliveira M J, Petri A and Tomé T, 2004 *Physica A* **342** 97
- [32] de Oliveira M J, Petri A and Tomé T, 2004 *Europhys. Lett.* **65** 20
- [33] Petri A, 2003 *Braz. J. Phys.* **33** 521
- [34] Ibáñez De Berganza M, Loreto V and Petri A, 2007 *Phil. Mag.* **87** 779
- [35] Lifshitz I, 1962 *Sov. Phys.—JETP* **15** 939
- [36] Safran S A, 1981 *Phys. Rev. Lett.* **46** 1581
- [37] Viñals J and Gunton J D, 1986 *Phys. Rev. B* **33** 7795
- [38] Viñals J and Grant M, 1987 *Phys. Rev. B* **36** 7036
- [39] Ibáñez de Berganza M, Ferrero E E, Cannas S A, Loreto V and Petri A, 2007 *Eur. Phys. J* **143** 273
- [40] Loureiro M P O, Aizenberg J J, Cugliandolo L F and Sicilia A, 2010 *Phys. Rev. E* **81** 021129
- [41] Loureiro M P O, Aizenberg J J and Cugliandolo L F, 2012 *Phys. Rev. E* **85** 021135
- [42] Glauber R J, 1963 *J. Math. Phys.* **4** 294
- [43] Bortz A B, Kalos M H and Lebowitz J L, 1975 *J. Comput. Phys.* **17** 10
- [44] Aizenberg J J, Bray A J, Cugliandolo L F and Sicilia A, 2007 *Phys. Rev. Lett.* **98** 145701
- [45] See the supplemental material at <http://physics.bu.edu/~redner/pubs/pdf/potts-sm.pdf>
- [46] Morris R, 2011 *Probab. Theory Relat. Fields* **149** 417
- [47] Fisher D S, 1997 *Physica D* **107** 204
- [48] Hoshen J and Kopelman R, 1976 *Phys. Rev. B* **14** 3438
- [49] Newman M E J and Ziff R M, 2000 *Phys. Rev. Lett.* **85** 4104